

# Experimental Determination of Asymmetry-Induced Trim Angles of Attack

EDWARD L. CLARK JR.\* and ALBERT E. HODAPP JR.†  
Sandia Laboratories, Albuquerque, N.Mex.

One- and three-degree-of-freedom dynamic stability balances were used in supersonic and hypersonic wind tunnels to measure the trim angles of attack of a  $10^\circ$  cone with small asymmetries. The asymmetries, tested independently, were a flare section near the base of the model and a misalignment of the principal axes with respect to the geometric axes. The test hardware, techniques, and results are described. Numerical simulations are compared with the wind tunnel results and full-scale flight data. The comparisons show that the trim angles determined with these techniques permit accurate prediction of flight performance.

## Nomenclature

$C_A$	= axial force coefficient
$C_{I_p}$	= roll damping derivative coefficient
$C_{m_q} + C_{m_{\dot{\alpha}}}$	= damping moment derivative coefficient
$C_{m_{\alpha}}$	= static moment derivative coefficient
$C_{N_{\alpha}}$	= normal force derivative coefficient
$d$	= vehicle reference (base) diameter
$I_X$	= axial moment of inertia
$I_Y, I_Z$	= lateral moments of inertia
$I_{XY}$	= product of inertia
$l$	= vehicle length
$l_w$	= trim wedge length (Fig. 1)
$M_\infty$	= freestream Mach number
$p$	= roll rate
$p_{cr}$	= critical roll rate, $\pm [-C_{m_q} q_\infty S d / (I_Z - I_X)]^{1/2}$
$q_\infty$	= freestream dynamic pressure
$S$	= vehicle reference (base) area
$t$	= time
$X_g, Y_g, Z_g$	= geometric axes (Figs. 1 and 7)
$X_p, Y_p, Z_p$	= principal axes (Fig. 7)
$\alpha_T$	= trim angle of attack
$\theta_w$	= trim wedge angle (Fig. 1)

## Introduction

THE Re-entry Vehicle Resonance Test Vehicle (RVRTV) flight program is a continuing study by Sandia Labs. to investigate roll-pitch coupling under simulated re-entry conditions. The rocket-boosted test vehicle is flown on a low-altitude supersonic Mach number trajectory which permits evaluation of ballistic re-entry vehicle behavior at a simulated second resonance, i.e., low-altitude resonance. The flight test technique is described in Ref. 1. The RVRTV configuration is a  $10^\circ$  half-angle cone with a nose-to-base radius ratio of 0.0167. The center of gravity of the vehicle is at 63% of the body length.

Two vehicles were flown at Sandia's Tonopah Test Range to examine, independently, the effects of an aerodynamic

asymmetry and an inertia asymmetry. The aerodynamic asymmetry was a small wedge (flare section) located at the aft end of the vehicle. The inertia asymmetry was generated by rotating two of the vehicle's principal axes with respect to the geometric axes. In both cases, the asymmetries were designed to provide a reference out-of-plane trim angle of  $0.5^\circ$  during the initial portion of the flight ( $M_\infty \approx 4.2$ ). The asymmetries were combined with an offset center of gravity so that the induced trim angle would produce a roll torque.

Success of these flights depended to a large degree on the accuracy with which the trim angle, induced by either type of asymmetry, could be predicted. During the planning phases of the flights, it was apparent that experimental determination of the trim angles, in a wind tunnel, would be advisable. The type of data desired, together with the small magnitude of the trim angles to be measured, required that new test hardware and procedures be developed. This paper presents the results of a study conducted to measure the trim angle of attack of a  $10^\circ$  cone with small asymmetries. Details of the experimental techniques, comparisons of experimental results with analytical and numerical predictions, and comparisons with flight data are presented in the following sections.

## Aerodynamic Asymmetry

### Experimental Technique

Desired accuracy of the trim angle measurement was  $\pm 0.05^\circ$ . To achieve this accuracy, it was felt that a differential measurement was necessary. That is, a technique must be used wherein the trim angle of the model is measured, with and without the asymmetry, during a single wind-tunnel run. Furthermore, a technique which permitted direct measurement of the trim angle was preferable to one wherein the trim angle was inferred, e.g., by measurement of pitching moment. These requirements were satisfied by supporting the model on a one-degree-of-freedom, bearing-type, dynamic stability balance, and by utilizing the following test procedures: the model, with asymmetry, was perturbed and permitted to damp to a steady-state attitude; the asymmetry was ejected by remote control; and the clean configuration was allowed to damp to a new steady-state attitude ( $\approx 0^\circ$ ). The difference in the two steady-state angles is the nonrolling (reference) trim angle of the vehicle.

The aerodynamic asymmetry tests were conducted in the 4-ft High Speed Wind Tunnel at Vought Aeronautics Company. In this tunnel, a 0.53-scale model with an 8.0-in (20.3-cm) base diameter could be tested at Reynolds numbers which were approximately one-half the flight values. The tests were conducted at Mach numbers of 1.6, 3.0, and 4.2 with freestream Reynolds numbers, based on model length, of

Received September 11, 1972; presented as Paper 72-1032 at the AIAA 7th Aerodynamic Testing Conference, Palo Alto, Calif., September 13-15, 1972; revision received December 13, 1972. This work was supported by the U.S. Atomic Energy Commission. The authors wish to acknowledge the assistance of E. W. Hall, E. J. Meyer, and T. T. Bramlette of Sandia Laboratories; L. K. Ward and A. C. Mansfield of ARO, Inc.; and J. W. Arnold of Vought Aeronautics Company.

Index categories: Re-Entry Vehicle Testing; Uncontrolled Rocket and Missile Dynamics.

\* Member of Technical Staff, Experimental Aerodynamics Division, Aerodynamics Research Department. Member AIAA.

† Member of Technical Staff, Aeroballistics Division, Aerodynamics Projects Department. Member AIAA.

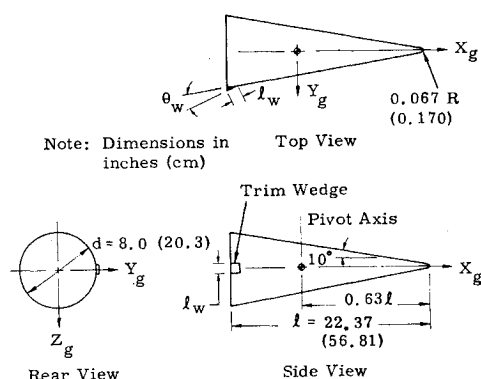


Fig. 1 Aerodynamic asymmetry model.

1.7, 2.3, and  $3.5 \times 10^7$ , respectively. With these test conditions, the boundary layer ahead of the asymmetry was turbulent, as it would be during the full-scale flight test, and accurate scaling of the results was possible.

The model details are shown in Fig. 1. The asymmetries tested were wedges (flare sections) which were square in planform and were flush with the base of the model; their dimensions are given in Table 1. The small wedges (Configurations 4S and 8S) were designed to produce a trim angle of  $0.3^\circ$  at  $M_\infty = 4.2$ , and the large wedges (4L and 8L) were designed to produce a trim angle of  $0.6^\circ$  at the same Mach number; thereby, the desired trim angle of the full-scale RVRTV was bracketed. Details of the wedge ejector mechanism are shown in Fig. 2. The wedge was held in place by the retaining and alignment pins until initial model oscillations were damped. The rotary solenoid was then energized to permit the retaining pin to be withdrawn and the wedge to be ejected by the spring-loaded plunger.

The dynamic stability balance had a one-degree-of-freedom ball bearing pivot located at 63% of the model length from the nose. The model was statically balanced about the pivot and was mounted in the tunnel with the pivot axis vertical to eliminate any effects of the slight model imbalance that would occur when the wedge was ejected. An eddy current-type angular transducer was incorporated in the balance to measure the angle of the model relative to a reference axis.

Table 1 Trim wedge configurations

Configuration	$\theta_w$ , deg	$l_w$ , in. (cm)
4S	4.0	1.070 (2.718)
8S	8.0	0.711 (1.805)
4L	4.0	1.519 (3.857)
8L	8.0	1.010 (2.565)

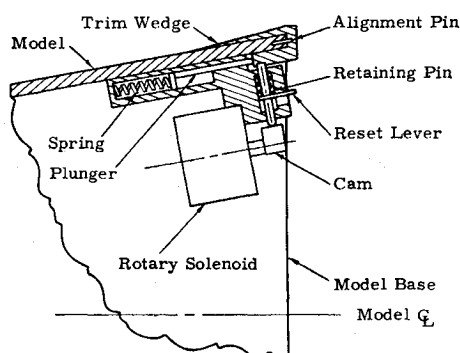
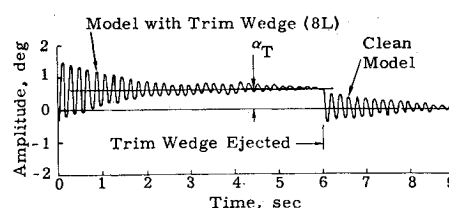


Fig. 2 Trim wedge ejector mechanism.

Fig. 3 Typical oscillogram from aerodynamic asymmetry test,  $M_\infty = 4.2$ .

### Wind-Tunnel Results

A typical oscillogram from a trim angle measurement is presented in Fig. 3. The advantages of this testing technique are apparent in the figure: 1) direct angle measurement; 2) instrumentation drift is not significant because of the "step" nature of the measurement; 3) instrumentation zero shifts, which cause uncertainty when two runs are required, are eliminated; and 4) effects of the slight differences in tunnel conditions which might occur between two runs are minimized.

A summary of the measured trim angles is presented in Fig. 4 where it can be seen that the measurements were repeatable. One run was made at  $M_\infty = 4.2$  with the model yawed  $0.5^\circ$  to simulate a roll-rate-induced flow angularity over the wedge. The effect of this small yaw angle was insignificant (Fig. 4). To permit accurate scaling and interpolation of the experimental results, the theory presented in Ref. 2 was developed. This theory assumes that viscous effects are negligible; therefore, the inviscid pressure on the wedge, corrected for aspect ratio effects, is used to predict the trim angle. The theoretical predictions, shown in Fig. 4, are in good agreement with the experimental measurements.

Although demonstrated for only a single type of asymmetry, the experimental technique can be extended to any aerodynamic asymmetry which can be generated or removed by remotely ejecting, retracting, extending, or rotating a section of the model.

### Flight Test Results

To verify that the present technique produced accurate trim angle measurements, numerical simulations based on the wind tunnel results are compared with flight test data. The flight test vehicle had mass and aerodynamic asymmetries built into it that were designed to produce a condition of persistent resonance during flight. The mass asymmetry was introduced by locating the center of gravity 0.101 in. (0.256 cm) below the centerline of the vehicle ( $X_g$  axis, Fig. 1) along the  $Z_g$  axis. The vehicle configuration was identical to the wind tunnel model (Fig. 1); however, the base diameter was larger, 15.0 in. (38.1 cm). The trim wedge was proportioned [ $\theta_w = 8.0^\circ$ ,  $l_w = 1.74$  in. (4.42 cm)] to produce a  $0.52^\circ$  out-of-plane nonrolling trim angle at Mach 4.2. The predicted

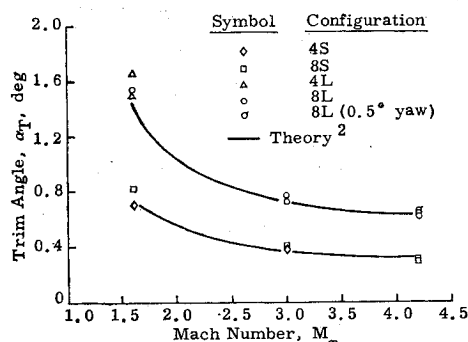


Fig. 4 Variation of trim angle with Mach number for model with aerodynamic asymmetry.

behavior of the flight test vehicle's nonrolling out-of-plane trim angle as a function of Mach number is given in Fig. 5. This prediction is based on the wind-tunnel results presented in Fig. 4.

In Fig. 6, roll rate and total angle-of-attack histories

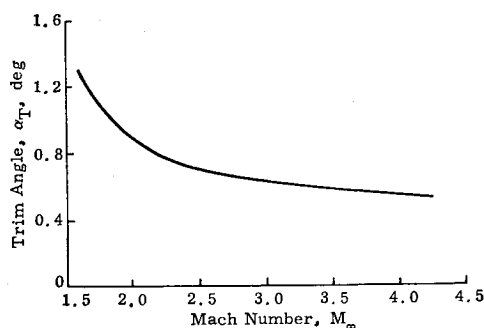


Fig. 5 Empirical prediction of trim angle for full-scale RVRTV with an aerodynamic asymmetry.

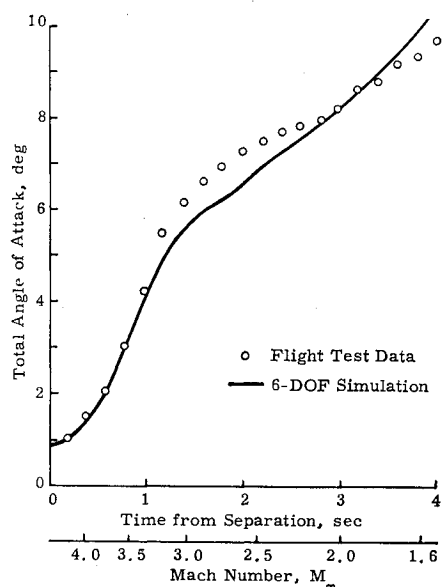
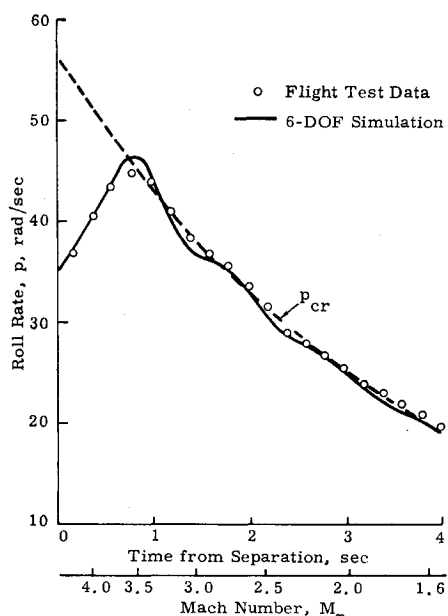


Fig. 6 Comparison of flight test results with 6-DOF simulation for RVRTV with an aerodynamic asymmetry.

obtained from a six-degree-of-freedom (6-DOF) simulation are compared with results obtained from the flight test. Under conditions of persistent resonance, the nonrolling trim angles caused by aerodynamic and mass asymmetries are greatly magnified. Note the good agreement between the simulated angular motion and that determined from the flight test. Since the nonrolling out-of-plane trim angle is the largest contributor to total angle of attack, these results indicate that the predicted trim angle-Mach number relationship given in Fig. 5 is a close approximation to the actual relationship.

## Inertia Asymmetry

### Experimental Technique

When the principal axes of a vehicle are not parallel with the axes of geometric symmetry, i.e., the aerodynamic axes, an inertia asymmetry exists. Since an inertia asymmetry may be generated without changing the external geometry of the vehicle, the aerodynamics of the vehicle are unaffected by the addition of the asymmetry. Although the dynamics of a vehicle with inertia asymmetries have been investigated recently,<sup>3</sup> at the time of the proposed flights 6-DOF numerical simulations were the only means of predicting the behavior of the vehicle; therefore, experimental verification of these simulations was desirable.

The trim angle induced by an inertia asymmetry is dependent on the vehicle's roll rate. Therefore, to investigate this type of asymmetry in a wind tunnel, it was necessary to use a support system which would permit three angular degrees of freedom (3-DOF). The von Kármán Gas Dynamics Facility at the Arnold Engineering Development Center (VKF-AEDC) was selected as the facility for this test because of the unique capabilities of the 3-DOF dynamic balance<sup>4</sup> which was developed at this facility. With this balance, the model was unrestrained in roll but was limited to a  $10^\circ$  total angle of attack. The balance incorporates variable reluctance transducers which provide roll rate data and continuous analog signals proportional to the nonrolling pitch and yaw angles.

Since the aerodynamics of the vehicle were of less interest than the dynamics, it was not necessary to match flight conditions, and the model could be tested in the 50-in. hypersonic Tunnel B where the model size and loads would be most compatible with the balance. The model was tested at a Mach number of 8 and a Reynolds number of  $2.9 \times 10^6$  based on model length. The boundary layer should be laminar over the entire model at these test conditions. The model was 0.67-scale with a base diameter of 10 in. (25.4 cm). The model center of rotation (i.e., the bearing center) was located at 55% of the body length and was offset 0.100 in. (0.254 cm) below the geometric centerline along the  $Z_g$  axis (Fig. 7).

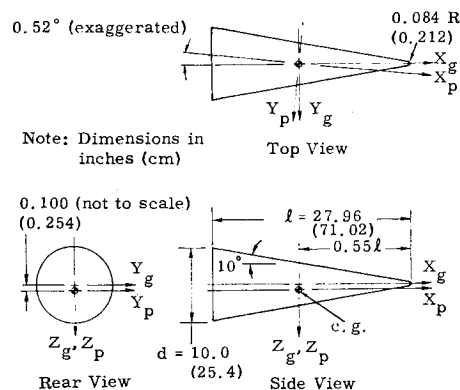


Fig. 7 Inertia asymmetry model.

Again, because exact scaling of the flight vehicle was not necessary for this test, the center of rotation was located at a longitudinal position which would permit direct comparison of the test results with data collected for this configuration at several facilities. Ballast was added to the model to locate the center of gravity at the center of rotation. After the ballast weights were installed in the model, the dynamic balance of the model was checked to insure that the principal axes were parallel with the geometric axes. An inertia asymmetry was then introduced by adding weights to the balanced model to produce a product of inertia,  $I_{xy}$ , which would give an out-of-plane principal axes inclination of  $0.52^\circ$  (Fig. 7). These weights were designed to maintain static balance about the center of gravity and to keep the lateral moments of inertia equal ( $I_y = I_z$ ).

The test procedure was to prespin the model to the desired initial roll rate by using a pair of air jets which impinged upon a turbine attached to the model. After the air jets were cut off, the angular motion of the model was unrestrained, and data were recorded.<sup>5</sup>

### Wind-Tunnel Results

The angular motions of a vehicle with an inertia asymmetry and an offset center of gravity are very dependent upon the ratio of roll rate to critical roll rate,  $p/p_{cr}$ , and the sign of the roll rate.<sup>3</sup> For the asymmetry combination used in the present test, a positive initial roll rate results in a roll acceleration which forces the model into a stable condition near resonance ( $p \approx p_{cr}$ ). On the other hand, a negative initial roll rate results in a roll acceleration which forces the model away from resonance. To evaluate the characteristic motions of the model under these conditions, four initial values of roll rate were selected; these values covered the full spectrum of roll behavior, i.e., subresonant ( $p/p_{cr} < 1$ ) and super-resonant ( $p/p_{cr} > 1$ ) conditions at positive and negative roll rates. Three runs were made at each initial roll rate, and repeatability of the data was excellent.

The roll rate histories are presented in Fig. 8 where the plotted points are average values from the three runs. The experimental results are compared with predictions obtained by numerically integrating the complete equations of motion for a rigid body with three angular degrees of freedom (3-DOF). The measured geometric and inertia properties of the model were used in the simulations. Aerodynamic coefficients were represented by theoretical estimates of  $C_A$  and  $C_{N_z}$ ; experimental values of  $C_{m_{\dot{\alpha}}}$  and  $C_{m_q} + C_{m_{\dot{\alpha}}}$  determined from

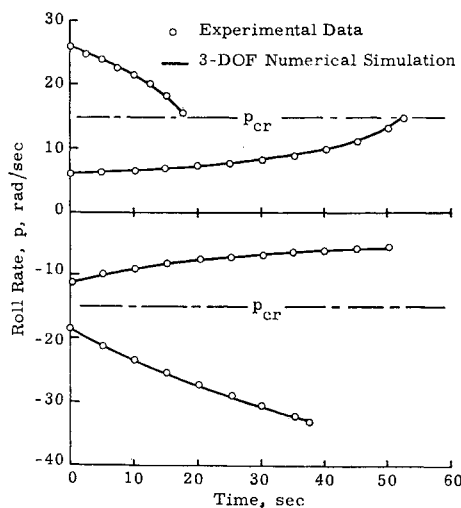


Fig. 8 Variation of roll rate with time for model with inertia asymmetry,  $M_\infty = 8$ .

a nonrolling, planar test of the asymmetrical model; and an experimental value of  $C_{l_p}$  determined with the symmetrical model (no inertia asymmetry or offset c.g.). Agreement between the numerical predictions and the experimental measurements of roll rate is excellent and indicates that the motion of a vehicle with inertia asymmetries can be accurately predicted with numerical simulations.

Significant transient angles of attack ( $2-5^\circ$ ) were introduced as the model was prespun through resonance; these transients, which were lightly damped, persisted throughout the super-resonant measurements. At conditions away from resonance, the roll torque associated with the transient angle of attack is oscillatory and has a mean value of nearly zero if the damping is small as in the present case. Hence, the transients do not significantly influence the roll histories. This was verified by 3-DOF simulations and also by observing that the roll rate data from the three repeat runs at each initial roll rate condition were in excellent agreement even though the transient angle behavior was different for each run.

Although transient angles of attack have little effect on these roll rate histories, they do prevent an immediate determination of the trim angle of attack. One method for separating the trim angle from the transient angle is to use an analysis based on the tricyclic solution of the linear differential equations of motion for a vehicle with small asymmetries.<sup>6</sup> This theory provides a means of representing the motion of a vehicle, in a nonrolling coordinate system, with three rotating modal vectors in the complex angle-of-attack plane. The transient angle of attack is given by two of the vectors, and the trim angle is given by the third. A nonlinear least-squares technique<sup>7</sup> was used to fit the pitch and yaw data to the tricyclic solution. The results of this analysis, presented in Fig. 9, are in good agreement with the 3-DOF numerical predictions. Near resonance ( $p \approx p_{cr}$ ), the measured trim angle may be slightly in error because of the difficulty in separating the magnitude of the trim modal vector from that of the transient (nutation) modal vector which has nearly the same angular frequency. It should be noted that the data shown in Fig. 9 include results from all four of the initial roll rates shown in Fig. 8.

The characteristic behavior of the trim angle induced by an inertia asymmetry is evident in Fig. 9. The trim angle has zero magnitude at  $p = 0$ , is magnified near resonance, and approaches the principal axis misalignment angle ( $0.52^\circ$ ) at large values of  $p/p_{cr}$ . Typically, response curves showing trim angle amplification as a function of roll rate are based on quasi-steady ( $dp/dt = 0$ ) calculations of the trim angle. The quasi-steady response of the trim angle, which was calculated by the method of Ref. 3, is shown in Fig. 9. The experimental data and the 3-DOF numerical calculations represent a dynamic condition with varying roll rate, and hence, lag the quasi-steady predictions near resonance where the roll acceleration is large.

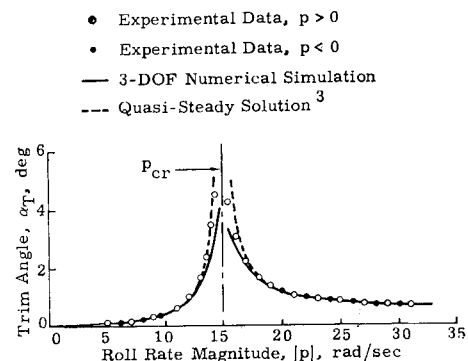


Fig. 9 Variation of trim angle with roll rate magnitude for model with inertia asymmetry,  $M_\infty = 8$ .

## Conclusions

From this experimental investigation of asymmetry-induced trim angles of attack, the following conclusions are drawn: 1) The trim angle of attack induced by certain types of aerodynamic asymmetries may be measured directly and accurately in a wind tunnel. For these tests, the magnitude of the trim angle was  $0.3\text{--}1.6^\circ$ , and the measurements were repeatable within  $\pm 5\%$ . Comparison of full-scale flight data with six-degree-of-freedom numerical simulations indicates that the trim angles determined with these techniques permit accurate prediction of flight vehicle performance. 2) The angular motions of a vehicle with an inertia-asymmetry-induced trim angle may be accurately reproduced in a ground test facility.

## References

<sup>1</sup> Hodapp, A. E., Jr. and Beckmann, R. C., "Flight Test Evaluation of a Fluidically Actuated Monopropellant Hydrazine Roll Control System," AIAA Paper 72-975, Palo Alto, Calif., 1972.

<sup>2</sup> Clark, E. L., Jr., "Trim Angle Predictions for a Slightly Blunted Conical Re-Entry Vehicle with a Flare-Section Asymmetry," SC-DR-72 0532, Sandia Labs., Albuquerque, N.Mex., to be published.

<sup>3</sup> Hodapp, A. E., Jr. and Clark, E. L., Jr., "Effects of Products of Inertia on Re-Entry Vehicle Roll Behavior," *Journal of Spacecraft and Rockets*, Vol. 8, No. 2, Feb. 1971, pp. 155-161.

<sup>4</sup> Ward, L. K., Jr. and Hodapp, A. E., Jr., "A Three-Degree-of-Freedom Dynamic Stability Balance for Use in the VKF Continuous Flow Hypersonic Tunnels ( $M_\infty = 6$  through 12)," AEDC-TR-68-62, May 1968, Arnold Engineering Development Center, Arnold Air Force Station, Tenn.

<sup>5</sup> Ward, L. K., Jr. and Mansfield, A. C., "Dynamic Tests of a 10-Deg Cone Having Three Angular Degrees of Freedom at Mach 8," AEDC-TR-69-151, Sept. 1969, Arnold Engineering Development Center, Arnold Air Force Station, Tenn.

<sup>6</sup> Nicolaides, J. D., "On the Free Flight Motion of Missiles Having Slight Configurational Asymmetries," Rept. 858, June 1953, Ballistic Research Lab., Aberdeen Proving Ground, Md.

<sup>7</sup> Eikenberry, R. S., "Analysis of the Angular Motion of Missiles," SC-CR-70-6051, Feb. 1970, Sandia Labs., Albuquerque, N. Mex.